J. Membrane Biol. 151, 149–157 (1996)

The Journal of
Membrane
Biology

K^+ Channels and the Intracellular Calcium Signal in Human Melanoma Cell Proliferation

A. Lepple-Wienhues[1], S. Berweck[1], M. Böhmig[1], C.P. Leo[1], B. Meyling[1], C. Garbe[2], M. Wiederholt[1]

[1]Institut für Klinische Physiologie, Universitätsklinikum Benjamin Franklin, Freie Universität Berlin, Hindenburgdamm 30, 12200 Berlin, Germany

[2]Dermatologische Klinik, Universitätsklinikum Benjamin Franklin, Freie Universität Berlin, Hindenburgdamm 30, 12200 Berlin, Germany

Received: 9 May 1995/Revised: 30 January 1996

Abstract. K^+ channels, membrane voltage, and intracellular free Ca^{2+} are involved in regulating proliferation in a human melanoma cell line (SK MEL 28). Using patch-clamp techniques, we found an inwardly rectifying K^+ channel and a calcium-activated K^+ channel. The inwardly rectifying K^+ channel was calcium independent, insensitive to charybdotoxin, and carried the major part of the whole-cell current. The K^+ channel blockers quinidine, tetraethylammonium chloride and Ba^{2+} and elevated extracellular K^+ caused a dose-dependent membrane depolarization. This depolarization was correlated to an inhibition of cell proliferation. Charybdotoxin affected neither membrane voltage nor proliferation. Basic fibroblast growth factor and fetal calf serum induced a transient peak in intracellular Ca^{2+} followed by a long-lasting Ca^{2+} influx. Depolarization by voltage clamp decreased and hyperpolarization increased intracellular Ca^{2+}, illustrating a transmembrane flux of Ca^{2+} following its electrochemical gradient. We conclude that K^+ channel blockers inhibit cell-cycle progression by membrane depolarization. This in turn reduces the driving force for the influx of Ca^{2+}, a messenger in the mitogenic signal cascade of human melanoma cells.

Key words: Melanoma cell line — Inward rectifying K^+ channel — Calcium-activated K^+ channel — Patch clamp — Intracellular calcium — Tumor cell proliferation — Basic fibroblast growth factor

Introduction

Melanoma is one of the most aggressive human cancers and shows increasing incidence in Western hemisphere countries. The tumor originates from neuroectodermal melanocytes which normally do not proliferate in the adult skin. The SK MEL 28 cell line has been established from a human cutaneous melanoma [5]. These cells are able to synthesize melanin, show anchorage-independent growth, induce tumors in nude mice, and have been well characterized by morphological and biochemical methods [30].

There is increasing evidence that membrane ion channels are involved in cell differentiation and cell-cycle control. In lymphocytes, activation of K^+ currents belongs to the early events following mitotic stimulation. K^+ channels provide the driving force for the rise in intracellular Ca^{2+} ($[Ca^{2+}]_i$) triggering T cell activation [4, 6, 8, 22]. Blockers of K^+ channels arrest lymphocytes in the early G_1 phase of the cell cycle [1]. The expression of K^+ channels changes with different mitotic phases [7]. K^+ channels interfere with proliferation in a variety of different cell lines derived from breast carcinoma [33], neuroblastoma [31], and renal epithelium [32].

Little is known about ion channels in melanoma cells. A ''delayed rectifier'' K^+ channel has been described in one melanoma cell line (IGR1) [25]. The proliferation of melanoma cells (SK MEL 28) is sensitive to external calcium and calmodulin antagonists and can be inhibited by K^+ channel blockers (IGR1) [14, 26, 27]. Autocrine secretion of basic fibroblast growth factor (bFGF) can enhance proliferation in a melanoma cell line [2], but the signaling pathways of bFGF in these cells remain unknown.

The present report characterizes the role of specific K^+ channels in melanoma cell proliferation, inhibition of cell growth by channel blockers, and mechanisms linking membrane K^+ conductance, intracellular free Ca^{2+}, and cell-cycle control. We focused on Ca^{2+}-independent and

Correspondence to: A. Lepple-Wienhues

Ca^{2+}-activated potassium channels and the $[Ca^{2+}]_i$ signal evoked by mitogens.

Materials and Methods

Cell Culture

SK MEL 28 cells were obtained from the Sloan Kettering Institute (New York). Cloned cells stemming from one single cell were cultured in RPMI 1640 medium supplemented with 10% fetal calf serum (FCS), 2 mM glutamine, 100 IU/ml penicillin, and 100 μg/ml streptomycin in a 95% air + 5% CO_2 atmosphere at 37°C. The cells were fed twice weekly. To synchronize the cells in an early phase of the cell cycle, all experiments were done using quiescent confluent cells 14–21 days after seeding. Cells were transferred to a small flow chamber immediately before experiments. When growth factors were used in experiments, the cells were kept without FCS for 48 hr.

Patch-clamp Experiments

Cells were allowed to attach to the bottom of a small perfusion chamber for 20 min. The chamber and the perfusate were heated to 37°C. Fluid exchange was tested by observing the voltage response to changes in extracellular K^+ ($[K^+]_e$) and was complete in less than 3 sec. Patch pipettes were pulled from borosilicate glass capillaries (Clark Elektromedical Instruments, Reading, GB) and polished using a DMZ puller (Zeitz Instrumente, Augsburg, FRG). Pipette resistances in Ringer's saline averaged 3–5 MΩ for whole-cell and 8–12 MΩ for single-channel recordings. For single-channel analysis, pipette capacity was reduced by silicone oil (200® Fluid, Dow Corning, La Hulpe, Belgium) layered upon the aqueous phase in the chamber [29]. An EPC9 patch-clamp amplifier (HEKA, Lambrecht, FRG) was used for voltage clamp and data acquisition. Data were sampled at 10 kHz (single-channel data) or 1 kHz (whole-cell data). We used REVIEW software (HEKA, Lambrecht, FRG) for analysis of whole-cell data (700 Hz filter) and the programs PATCH (A. Rabe, Frankfurt/M., FRG) and TAC (HEKA, Lambrecht, FRG) for single-channel data analysis (1 kHz filter). Recordings containing more than 200 events were used for statistical analysis. To determine time constants, more than 1,000 events were analyzed. Membrane capacitance (28 ± 1.5 pF) and access resistance (9.6 ± 0.7 MΩ) were monitored during whole-cell experiments (n = 132) using the C_{slow} update feature of the EPC9. The corresponding values with perforated patches were 25 ± 5.2 pF and 17 ± 6.3 MΩ (n = 17), respectively. According to convention, all voltages are given relative to the electrode at the outside of the cell membrane, and positive current means flow of positive charges from inside to outside.

Cell-proliferation assay

The fluorescent dye 4-methylumbelliferyl-heptanoate (MUH) is converted into its fluorescent form only in viable cells [9]. Therefore the dye provides an excellent tool to determine cell numbers. Fluorescence intensity has been shown to linearly correlate with the number of SK MEL 28 cells assayed by thymidine incorporation or visual cell counting [14]. The cells were plated in 96-well microtiter plates at a density of 10^4 cells/well. RPMI medium containing K^+ channel blockers or elevated K^+ was added two days after seeding. All values were normalized to controls treated with RPMI medium containing 5% FCS only. On day 5, cells were incubated for 1 hr in phosphate buffered saline containing 10^{-4} M MUH. Fluorescence was measured using a Titertec Fluoroscan II (Flow Laboratories, Meckenheim, Germany). The data represent means ± SEM of 1–5 experiments, and every assay was performed 6-fold in each experiment.

Measurement of Intracellular free Ca^{2+}

Intracellular free Ca^{2+} was measured in single cells at 37°C using the dye fura-2 [13]. Cells were either loaded with 10^{-4} M fura-2 pentapotassium salt via the patch pipette or, for long-term recordings, in RPMI medium containing 10 μM fura-2-acetoxymethylester (60 min., 20°C). Dual-wavelength photometry was done either using a Fura-2 Data Acquisition System (Max Plank Institut für Biophysikalische Chemie, Göttingen, FRG) or with a Spex DM 3000 CM spectrofluorometer (Spex Industries, NJ). The fluorescence data were analyzed using a personal computer as described elsewhere [28].

Solutions and Chemicals

The standard external solution for all experiments contained (all values in mM): 151 Na^+, 5 K^+, 1 Mg^{2+}, 1.7 Ca^{2+}, 158 Cl^-, 1 SO_4^{2-}, 1 $H_2PO_4^-$, 10 HEPES, 5 glucose (pH 7.4). For whole-cell patch-clamp recordings the internal solution contained 135 K^+, 10 Cl^-, 125 methanesulphonate$^-$, 10 HEPES, 10 EGTA, and 1 MgATP (pH 7.2). For single-channel analysis the bath solution contained 150 K^+, 150 Cl^-, 10 HEPES, and 10 EGTA (pH 7.2). The pipette solution contained 150 K^+, 153 Cl^-, 10 HEPES and 1.7 Ca^{2+} (pH 7.4). Free Ca^{2+} in internal solutions was varied using a Ca^{2+}-saturated EGTA solution as described [24] and buffered to 3×10^{-7} M unless otherwise indicated. In experiments with variable potassium concentrations, K^+ was replaced by Na^+. For perforated patch experiments, a stock solution of nystatin in dimethylsulfoxide was prepared and diluted 1:1000, yielding a final nystatin concentration of 100 μg/ml. The tips of the pipettes were then filled with nystatin-free solution and backfilled with the nystatin-containing solution. In some experiments methanesulphonate$^-$ replaced Cl^- in order to exclude Cl^- currents (*not shown*). Cell culture media were purchased from Biochrom (Berlin, FRG), charybdotoxin (CTX) from Alomone Labs (Jerusalem, Israel) and recombinant human bFGF from Bachem (Bubendorf, Switzerland). All other chemicals were obtained from Sigma (Deisenhofen, FRG).

Results

Single-channel Currents

Cell-attached K^+ Channels

We observed 2 different K^+-channels (Fig. 1 *a* and *b*). The first channel was inwardly rectifying (K_{IR}). This channel showed an open probability (p_o of 58 ± 8.4% in the cell attached mode and was seen in 14% of all patches. It probably mediated the main resting K^+ conductance in these melanoma cells. A second, faster gating channel (K_{Ca}) was present in 30% of the patches with a low p_o in the attached mode (1.8 ± 0.6%). This channel was routinely activated by excising the patch into Ca^{2+}-containing solutions (Fig. 1 *a, see below*).

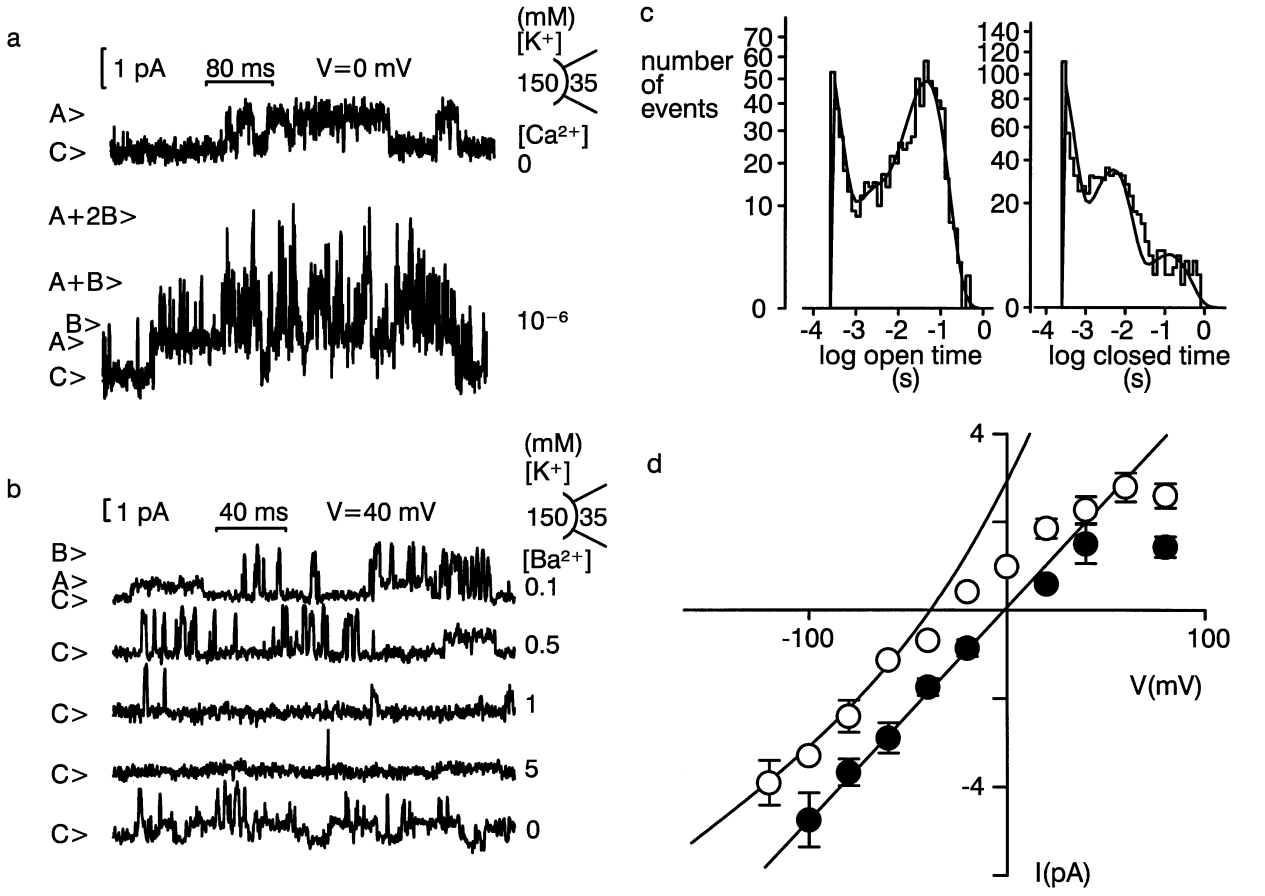

Fig. 1. Two different K^+ channels in an excised inside-out patch. (*a*) The slower gating channel (K_{IR}) opens in the absence of Ca^{2+} in the bath (10 mM EGTA), the faster gating channel (K_{Ca}) is activated by addition of Ca^{2+}. C> indicates closed level, A> opening of the K_{IR} and B> (2B>) opening of 1 (2) K_{Ca} channels. (*b*) Typical traces of a patch containing both channels, which are both reversibly blocked by addition of Ba^{2+} to the bath. The lowest trace shows recovery of the channel activity after wash. (*c*) Open-time and closed-time distribution of a K_{IR} channel in an excised inside-out membrane patch at −80 mV ($[K^+]_i = [K^+]_e$ = 150 mM) showing the number of open and closed events on a square root transformed ordinate. Exponentials are fitted to the data. Time constants were 0.167 msec, 1.9 msec, and 51.1 msec for the open-time and 0.194 msec, 5.5 msec, and 141 msec for the closed-time distribution. (*d*) Current voltage relation of excised K_{IR}-channels (● measured with 150 mM symmetrical K^+, ○ with $[K^+]_i/[K^+]_e$ = 150/35 mM, n = 3–5). The lines fit data points below −10 mV to the Goldmann-Hodkin-Katz equation demonstrating single-channel inward rectification.

The K_{IR} Channel

In excised inside-out patches the single-channel currents showed inward rectification (Fig. 1*d*). The slope conductance determined from the linear portion of the inward current averaged 45 pS ($[K^+]_i/[K^+]_e$ = 150/150 mM) and 31 pS ($[K^+]_i/[K^+]_e$ = 150/35 mM). The gating of K_{IR}-channels was characteristically slow. Mean open times were 30.0 ± 11.3 msec at 40 mV and 21.3 ± 9.8 msec at −40 mV (Fig. 1*c*).

Due to unstable patches at positive holding potentials, we reduced $[K^+]_e$ to test for ionic selectivity. The reversal potential shifted <−30 mV when the pipette contained 35 mM instead of 150 mM K^+ (Fig. 1*d*) and whole cell currents at different external potassium concentrations showed a high selectivity for K^+ over Na^+ (*see below*).

Neither p_o nor gating characteristics of the channel were altered when the internal $[Ca^{2+}]$ was withdrawn and 10 mM EGTA was added (mean open time = 26.2 ± 13.1 msec, n = 4, Fig. 1*a*). Internal Ba^{2+} blocked the channel in excised inside-out patches (n = 3, Fig. 1*b*). Backfilling the pipette with 5 mM Ba^{2+} completely blocked the initial channel activity within 2–5 min; CTX (10^{-7} M) had no effect (n = 3, n = 4, *not shown*). Without blockers in the pipette, channel activity remained stable for up to 20 min.

The K_{Ca} Channel

This channel had flickering kinetics (mean open time 1.02 ± 0.2 msec) and could therefore be easily distinguished from the K_{IR} channel (Fig. 1*a*, and *b*). It was activated by excision into a Ca^{2+}-containing solution

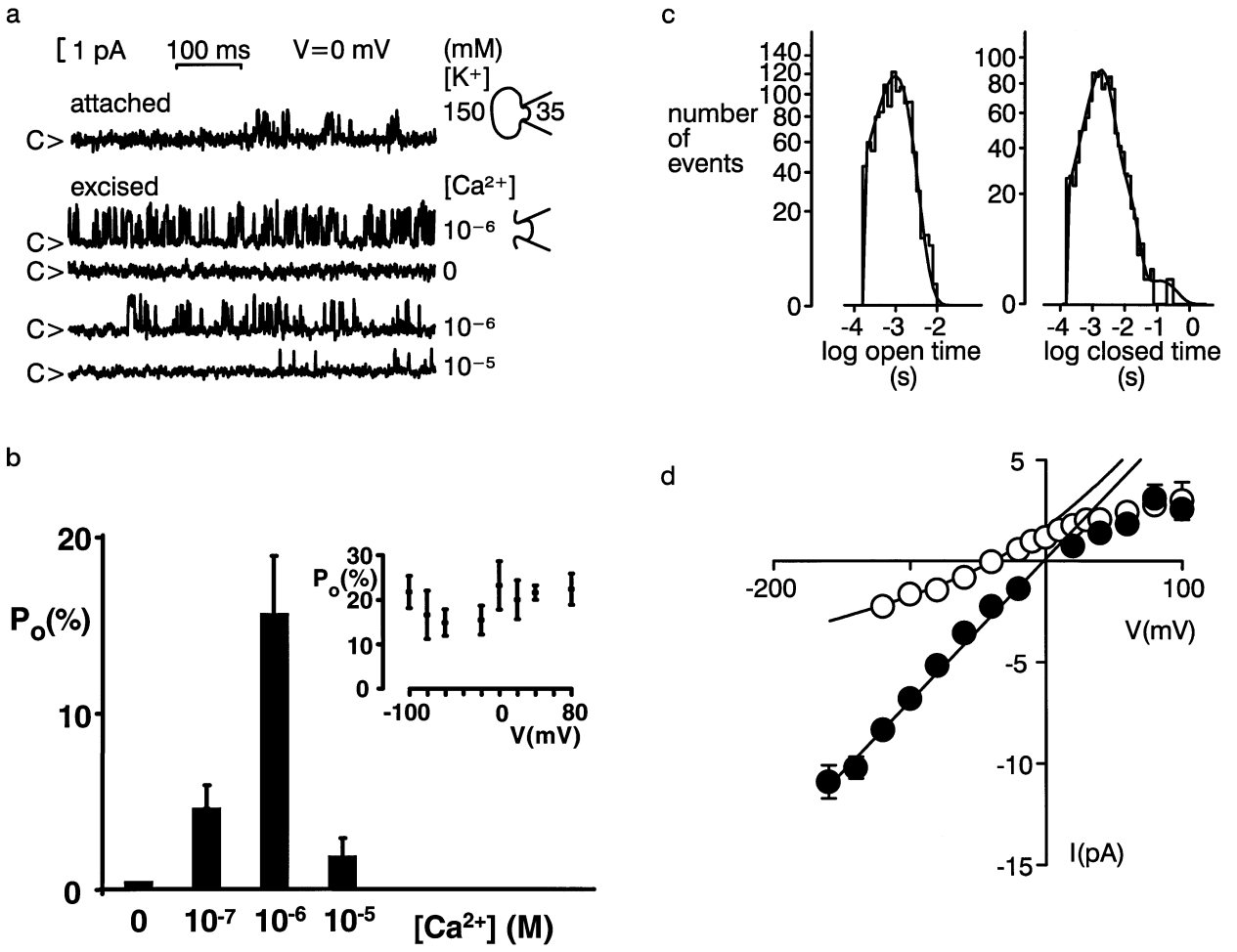

Fig. 2. Attached and excised inside-out patches containing the K_{Ca} channel. (*a*) Typical records showing the dependence of channel activity on $[Ca^{2+}]_i$. Note the channel block by 10^{-5} M $[Ca^{2+}]$. (*b*) Open probability as a function of $[Ca^{2+}]_i$ in excised patches containing the K_{Ca} channel ($n = 5$). The inset shows open probabilities at different holding potentials ($[K^+]_i/[K^+]_e$ = 150/35 mM, $[Ca^{2+}]_i = 10^{-6}$ M, n = 3–5). (*c*) Open-time and closed-time distribution of a K_{Ca} channel in an excised inside-out membrane patch at 40 mV ($[K^+]_i = [K^+]_e$ = 150 mM). *See also* legend to Fig. 1*c*. (*d*) Current/voltage relation of excised K_{Ca}-channels (● measured with 150 mM symmetrical K^+, ○ with $[K^+]_i/[K^+]_e$ = 150/35 mM, n = 4–10). *See also* legend to Fig. 1*d*.

(Fig. 2*a*). No correlation was apparent between p_o and the holding voltage (Fig. 2*b*). With 10^{-6} M Ca^{2+} in the bath, the open-time distribution was fit using a single exponential, yielding a time constant of τ = 1.09 msec (Fig. 2*c*).

The *I/V* relation of the K_{Ca} channel also showed inward rectification (Fig. 2*d*). The linear portion of the *I/V* relation gave unitary slope conductances of 73 pS ($[K^+]_i/[K^+]_e$ = 150/150 mM) and 29 pS ($[K^+]_i/[K^+]_e$ = 150/35 mM). The K_{Ca} channel was highly selective for K^+ over Na^+. The reversal potential shifted <−35 mV when $[K^+]_e$ was reduced ($[K^+]_i/[K^+]_e$ = 150/35 mM).

P_o was strongly Ca^{2+}-dependent. Maximal activation was reached at 10^{-6} M, and further increases of $[Ca^{2+}]_i$ elicited a channel block at 10^{-5} M (Fig. 2*b*). When the cytosolic side of the excised channel faced 10^{-7} M $[Ca^{2+}]$, channel activity was comparable to the cell-attached configuration.

Ba^{2+} blocked the channel dose dependently when added to the bath (n = 3, Fig. 1*b*). Backfilling the pipette with tetraethylammonium chloride (TEA, 10 mM, n = 3), Ba^{2+} (5 mM, n = 3), and CTX (10^{-7} M, n = 8) blocked the initial channel activity within 2–5 min. (*not shown*). No rundown of channel activity was observed without blockers in the pipette solution.

Whole-cell Currents

Perforated-patch vs. Conventional Whole-cell Recording

The perforated-patch technique allows electrical access to the cell with minimal perturbance of cytosolic components. Access was obtained within 5–15 min. The membrane voltage measured immediately after establish-

ing electrical access was −52 ± 5 mV in 17 perforated patches, and −56 ± 3 mV using conventional whole-cell, recordings ($n = 30$). The reversal potential shifted to more negative values after conventional break-in, possibly indicating rundown of a leak conductance. Currents in standard Ringer's and elevated $[K^+]_e$ solutions and inhibition by external Ba^{2+} were similar with both perforated and conventional whole cell recording techniques (*not shown*). Therefore, conventional whole-cell techniques were used for the following studies.

I/V Relation of Whole-cell Currents

The whole-cell current of resting cells was inwardly rectifying. Using voltage steps from a holding potential of −60 mV, current activation was fast and complete within the capacitive transient. No inactivation could be observed with voltage steps lasting for up to 400 msec (Fig. 3*a*).

The current was further characterized using voltage ramps from −120 to 60 mV of 1-sec duration. Each ramp was preceded by a set of small pulses for series resistance and capacitance compensation. The reversal potential increased 60 mV per tenfold change of $[K^+]_e$ (Fig. 3*b* and *c*), indicating a high selectivity of the current for K^+ over Na^+. Simultaneously, the threshold voltage for inward rectification shifted to more positive potentials and the conductance increased.

Growth Factors Increase K^+ Conductance

Application of bFGF (100 μg/l) induced fast transient changes of the whole-cell current. The conductance increased 10–20 fold and the reversal potential shifted towards more negative values in 3 out of 13 cells (23%). The same effect was seen using FCS (10 vol.%) in 18 out of 23 cells (78%). Unresponsive cells showed no change in conductance. A typical time course of the transient outward current and reversal potential after stimulation with FCS is presented in Fig. 3*d*. The current transient was reversibly blocked by 50 nM CTX ($n = 3$, Fig. 3*e*), indicating activation of the K_{Ca} channel. The membrane capacitance remained unchanged (*not shown*).

In some experiments, we included guanosine 5′-0-(2-thiodiphosphate) (GDP-β-S, 10^{-5} M, $n = 9$) in the pipette solution. We observed no change of membrane current induced by diffusion of this compound into the cytosol and the response to 10% FCS remained unchanged.

K^+ Channel Blockers

Ba^{2+} and Cs^+ blocked the current at IC_{50} values of 2.3 and 0.3 mM, respectively (−60 mV, $n = 4$–6). The block was voltage dependent (*not shown*). Block by TEA and quinidine was not voltage dependent. IC_{50} values were 12 mM for TEA and 0.02 mM for quinidine ($n = 5$–6, *not shown*).

Contribution of the K_{Ca} channel to the resting whole-cell K^+ conductance was tested using the specific blocker CTX. Only a small portion of the whole-cell current was inhibited by CTX ($IC_{50} = 4 \times 10^{-9}$ M; $n = 5$, *not shown*). This was presumably due to the low open probability of the K_{Ca} channel seen in attached patches.

Ba^{2+}, TEA, and quinidine depolarized the reversal potential in a K^+ gradient ($[K^+]_e/[K^+]_i = 135/5$ mM), whereas CTX evoked only a small depolarization. The effects on reversal potential are summarized in Fig. 4*a* ($n = 5$–6).

Apamin (10^{-6} M, $n = 5$), a blocker of small Ca^{2+}-activated potassium channels, had no effect. Neither the K^+ channel openers diazoxide (10^{-6} M, $n = 3$) and minoxidil (10^{-5} M, $n = 3$) nor the blocker of ATP-sensitive K^+ channels, gibenclamide (10^{-6} M, $n = 3$), had any measurable effect on the whole-cell current (*not shown*). The muscarinic agonist carbachol (10^{-5} M, $n = 8$) and the β-adrenergic agent isoproterenol (10^{-5} M, $n = 6$) had no effect.

Cell Proliferation

Melanoma cell proliferation was blocked by TEA, quinidine, Ba^{2+}, and increased extracellular K^+. CTX did not inhibit proliferation. Figure 4*b* demonstrates the correlation between membrane depolarization and proliferation block. Depolarization to a potential more positive than −45 mV inhibited cell growth. TEA was slightly more potent in inhibiting growth than depolarizing the membrane, probably indicating a nonspecific effect of this drug on proliferation. No cytotoxic effects were seen in confluent and proliferating cell layers using trypan blue exclusion. Following washout of the blocking agents proliferation resumed at a normal rate (*not shown*).

Intracellular Free Calcium, $[Ca^{2+}]_I$

The mitogens bFGF and FCS induced a short peak in $[Ca^{2+}]_i$ followed by a sustained increase. A typical recording is shown in Fig. 5*a*. During the sustained phase, removal of $[Ca^{2+}]_e$ reduced $[Ca^{2+}]_i$ to resting levels. Readdition of $[Ca^{2+}]_e$ was followed by an overshooting recovery of $[Ca^{2+}]_i$, indicating an increased Ca^{2+}-influx (Fig. 5*a*). Similar responses were seen in 3 out of 5 cells using 10% FCS (60%) and in 6 out of 13 cells (46%) using 100 μg/l bFGF. A further calcium increase was frequently observed after a time delay of 10–20 min and some cells developed $[Ca^{2+}]_i$ fluctuations. The initial peak was also seen in the absence of external calcium, indicating a calcium release from intracellular stores (Fig. 5*b*). This peak paralleled the observed transient

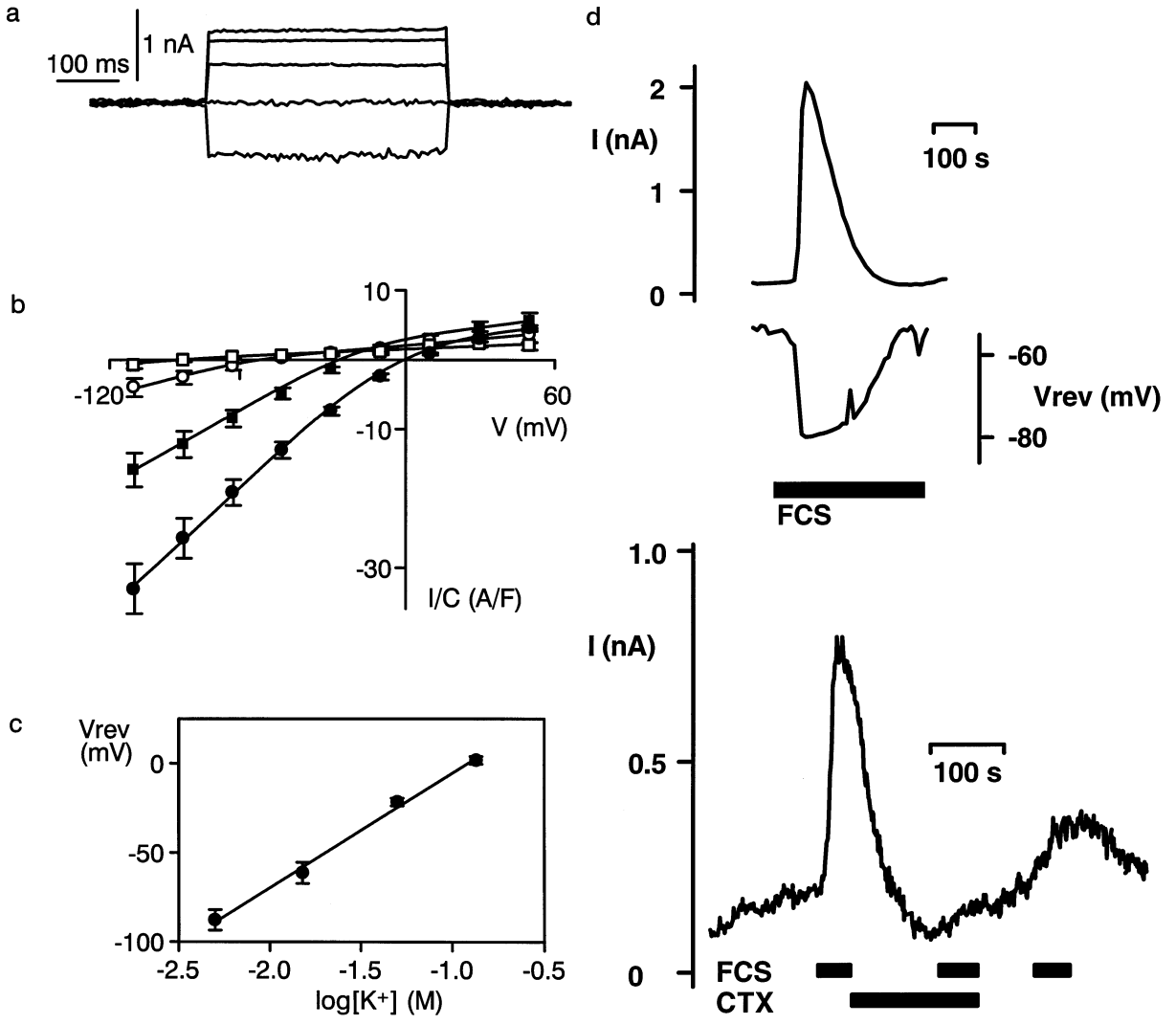

Fig. 3. (*a–c*) Whole-cell currents of SK MEL 28 melanoma cells. (*a*) Current response to voltage steps from −60 mV to −100, −60, −20, 20 and 60 mV, showing fast activation and no inactivation ($[K^+]_e = [K^+]_i = 135$ mM). (*b*) Current/voltage relation of whole-cell currents obtained by voltage steps ($[K^+]_e = 5$ (□), 15 (○), 50 (■), 135 (●) mM, $[K^+]_i = 135$ mM, $n = 5$). (*c*) Reversal potential is plotted *vs.* the extracellular K^+ concentration ($n = 5$). (*d*) Whole-cell conductance increases and reversal potential hyperpolarizes after application of 10% FCS, indicating the transient activation of a K^+ current. Outward current at 30 mV and reversal potential were measured using voltage ramps. (*e*) Outward current transients induced by a short application of 10% FCS can be blocked with 50 nM CTX. Note the partial recovery after CTX removal. Repetitive transients could be evoked in the absence of CTX when short FCS pulses were used ($n = 3$, *not shown*).

rise of K^+ conductance as expected for activation of the Ca^{2+}-activated K^+ channel (Fig. 3*d*, *e*). Depolarizing the membrane using elevated $[K^+]_e$ reduced calcium levels (Fig. 5*c*, $n = 15$). The sustained calcium rise could be reversed by removal of FCS (Fig. 5*c*, $n = 13$).

To further test whether the Ca^{2+} influx is dependent on membrane voltage, we measured $[Ca^{2+}]_i$ in the whole-cell configuration loading cells via the pipette with fura-2. At −90 mV $[Ca^{2+}]_i$ increased (Fig. 5*d*), indicating a transmembrane flux of Ca^{2+} following its electrochemical gradient. At 40 mV $[Ca^{2+}]_i$ decreased towards the buffered level of the pipette solution. Similar results were obtained in 5 cells.

Discussion

This study describes for the first time an inwardly rectifying K^+ channel and a CTX-sensitive, Ca^{2+}-activated K^+ channel in a human melanoma cell line. Block of the inwardly rectifying K^+ channel inhibits cell proliferation. Growth factor signaling includes a sustained rise in $[Ca^{2+}]_i$ and calcium influx is inhibited by depolarization.

Cell cycle-related signaling has been studied most extensively in lymphocytes. Their membrane voltage is maintained by a voltage-activated K^+ channel. Proliferation of T lymphocytes can be abolished by peptides specifically blocking this channel [19]. This action of K^+

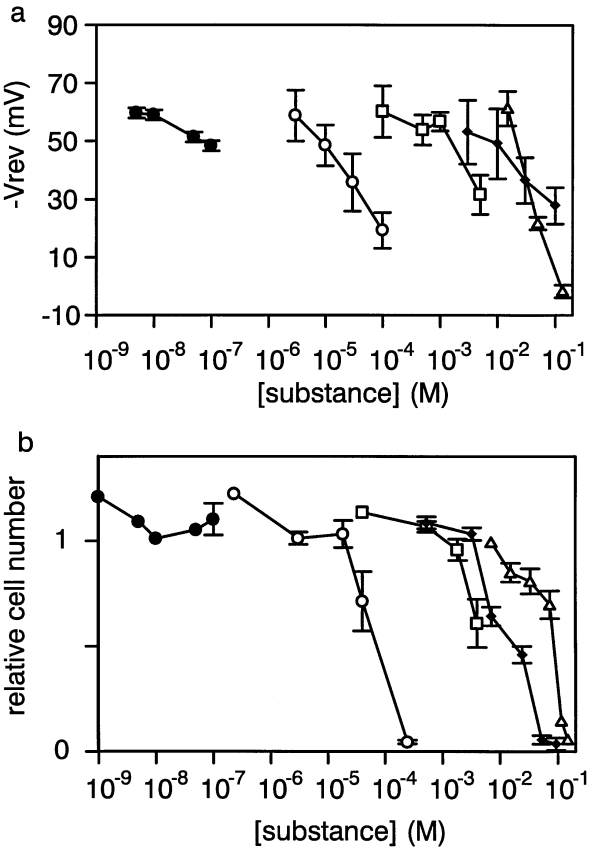

Fig. 4. Different K^+ channel blockers and elevated external K^+ depolarize the resting membrane potential and inhibit cell proliferation. (*a*) Membrane voltage is plotted against concentration (● CTX, ❍ quinidine, □ Ba^{2+}, ♦ TEA, △ K^+). The voltage was obtained from the reversal potential of the whole-cell current using voltage ramps. (*b*) Number of cells in proliferation assays is normalized to control and plotted against drug concentration (same symbols as in *a*).

channel blockers is restricted to activation pathways which involve a rise in intracellular Ca^{2+} [23]. T lymphocytes also possess a Ca^{2+}-activated K^+ channel inhibitable by CTX, but this channel is not necessary for cell activation [11, 12]. The early Ca^{2+} signal in lymphocytes induces a series of intracellular biochemical events including the transcriptional activation of several protoonocogenes. An increase of $[Ca^{2+}]_i$ activates calcineurin, the translocation of the transcriptional factor NF-IL2A, the MAPII kinase, and DNA synthesis-promoting factor (reviewed in [3]).

K^+ Channels and Proliferation

In SK MEL 28 melanoma cells, K^+ channel blockers which depolarized the membrane inhibited proliferation. The effect on proliferation was not linked to a reduced K^+ turnover, as shown by elevating $[K^+]_e$. As in lymphocytes, specific inhibition of the K_{Ca} channel was not sufficient to depolarize membrane voltage and inhibit cell growth.

We found two different K^+ channels. The activity of the K_{Ca} channel was low in resting cells. The membrane voltage was mainly determined by the K_{IR} channel and a putative depolarizing leak conductance. In melanoma cells the main K^+ conductance was not sensitive to CTX.

The K_{IR} channel described here had slow gating kinetics at 37°C, was blocked by Ba^{2+}, and its conductance was dependent on $[K^+]_e$. When compared to other inwardly rectifying channels, this channel was markedly less sensitive to external Ba^{2+}. Inwardly rectifying channels have been found in different excitable and nonexcitable cells including Hela tumor cells (for review *see* [16]). At membrane voltages positive to the potassium equilibrium potential, inwardly rectifying K^+ channels can avoid a high K^+ turnover.

The K_{Ca} channel resembled a typical Ca^{2+}-activated potassium channel, with intermediate conductance sensitive to CTX, but not apamin. It also showed typical flickering kinetics, which have been described in several cell types [16, 18]. This channel could be involved in the regulation of $[Ca^{2+}]_i$. Ca^{2+}-mediated hyperpolarization increases the electrochemical force for Ca^{2+} influx, thus providing a positive feedback mechanism. On the other hand, the channel was blocked by very high Ca^{2+} concentrations as described for high conductance K^+ channels [10].

In contrast to the IGR1 melanoma cell line [25], voltage activated K^+ channels are not expressed and isoproterenol does not regulate K^+ currents in SK MEL 28 cells.

$[Ca^{2+}]_i$ and Growth Factors

The $[Ca^{2+}]_i$ response to growth factors was biphasic. BFGF and FCS induced an early increase of K^+ conductance and elevated $[Ca^{2+}]_i$ resembling the mechanisms of lymphocyte activation. This represents most probably activation of the Ca^{2+}-activated K^+ channels by release of Ca^{2+} from intracellular stores [3]. The second, sustained elevation of $[Ca^{2+}]_i$ increased after 10–20 min. This $[Ca^{2+}]_i$ plateau phase was dependent on extracellular Ca^{2+}. Both the overshooting Ca^{2+} rise after readdition of extracellular Ca^{2+} and the inhibition of Ca^{2+} influx by depolarization point to a capacitive Ca^{2+} entry mechanism. Ca^{2+} entry through capacitive Ca^{2+} channels depends on membrane polarization in mast cells and lymphocytes [15, 17, 34]. In melanoma cells, we demonstrated a Ca^{2+} influx increasing at negative membrane voltages. Because of the high K^+ conductance we were unable to resolve the Ca^{2+} current in patch-clamp experiments. Cell cycle-dependent expression of receptors or arbitrary washout of signal cascade components could explain why only a subset of cells responded to growth

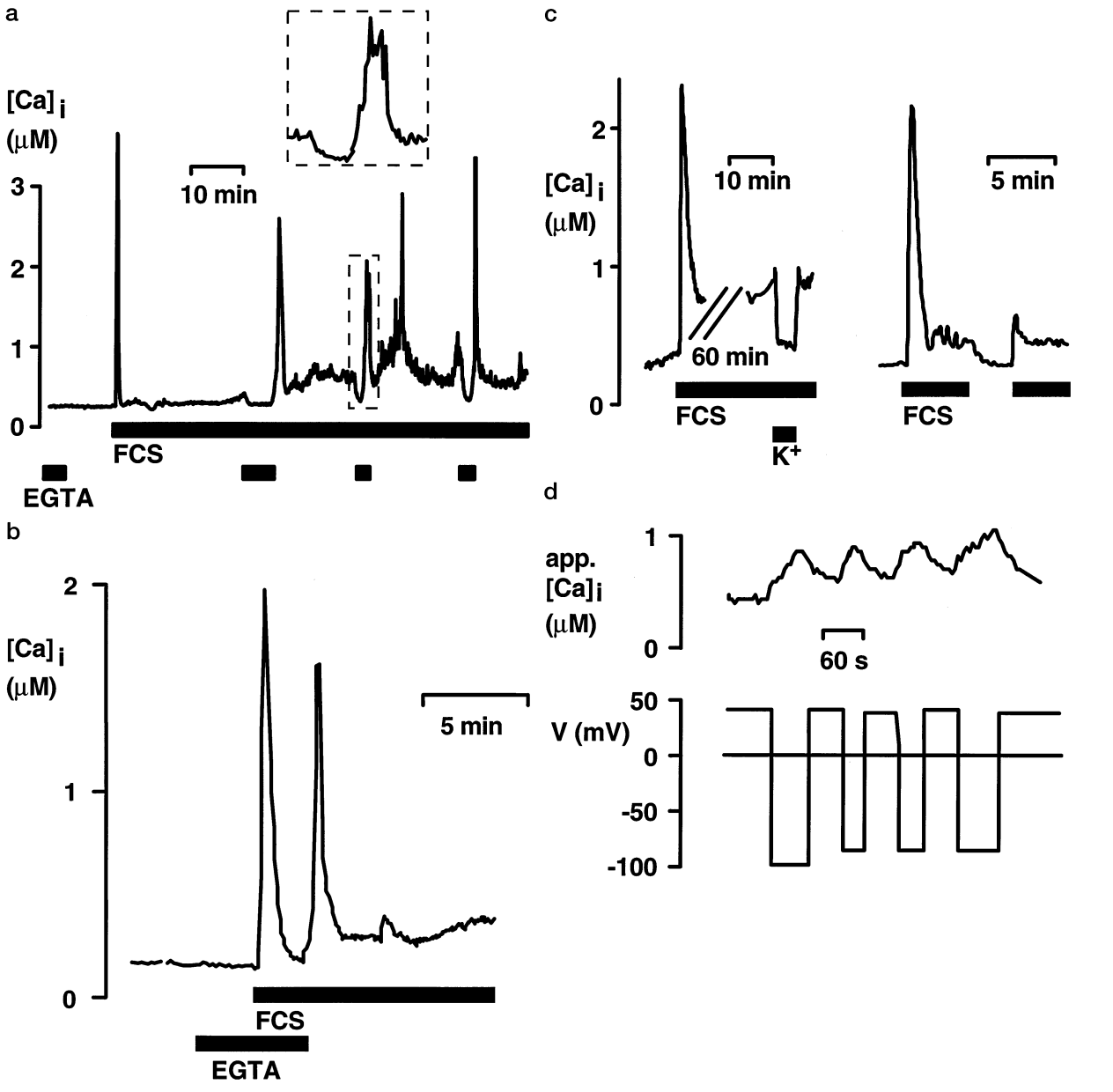

Fig. 5. Growth factors increase $[Ca^{2+}]_i$. (*a*) Long-term recording from a single melanoma cell loaded with fura2-acetoxymetylester showing the typical biphasic increase of intracellular Ca^{2+}. Bars indicate addition of 10% FCS and 10 mM EGTA. The sustained $[Ca^{2+}]_i$ elevation depends on extracellular calcium. Note the fluctuations and the overshooting response following readdition of Ca^{2+}. The inset shows the response to Ca^{2+} removal at a magnified time scale. (*b*) Internal store release is demonstrated by application of FCS in the absence of external Ca^{2+}. The initial calcium transient is independent of extracellular Ca^{2+}. (*c*) During the sustained Ca^{2+} rise, membrane depolarization by elevated $[K^+]_e$ brings $[Ca^{2+}]_i$ back to baseline (left panel). $[Ca^{2+}]_i$ returns to control levels when external FCS is removed as shown in a different cell (right panel). (*d*) Response of $[Ca^{2+}]_i$ to changes in membrane voltage. The cell was loaded with 10^{-4} M fura-2-pentapotassium salt via the pipette, and the membrane potential was changed by voltage clamp.

factors. However, we observed no correlation between access resistance and response to bFGF or FCS. Growth inhibition by depolarization is most probably due to the secondary block of a $[Ca^{2+}]_i$ elevation necessary for entering the cell cycle. K^+ channel block seems to inhibit the cell cycle by interference with the intracellular Ca^{2+} signal in different cell lines expressing various K^+ channel types. Inhibition of K^+ channels and Ca^{2+} fluxes represents a possible means to specifically inhibit tumor cell proliferation.

The expert assistance of Mrs. A. Krolik and Mrs. M. Boxberger is gratefully appreciated. We thank Ruth and Michael Cahalan and Paul Ross for their valuable comments on this manuscript. Part of this work

has been published in abstract form [20, 21]. This work was supported by the Deutsche Forschungsgemeinschaft (DFG Wi 328/11 and DFG Le 792/2-1).

References

1. Amigorena, S., Choquet, D., Teillaud, J., Korn, H., Fridman, W.H. 1990. Ion channel blockers inhibit B cell activation at a precise stage of the G1 phase of the cell cycle. *J. Immunol.* **144:**2038–2045
2. Becker, D., Meier, C.B., Herlyn, M. 1989. Proliferation of human malignant melanomas is inhibited by antisense oligodeoxynucleotides targeted against basic fibroblast growth factor. *EMBO J.* **8:**3685–3691
3. Berridge, M.J. 1993. Inositoltrisphosphate and calcium signaling. *Nature* **361:**315–325
4. Brent, L.H., Butler, J.L, Woods, Jr. W.T., Bubien, J.K. 1990. Transmembrane ion conductance in human B lymphocyte activation. *J. Immunol.* **145(8):**2381–2389
5. Carey, T.E., Takahashi, T., Resnick, L.A., Oettgen, H.F., Old, L.J. 1976. Cell surface antigens of human malignant melanoma: Mixed hemadsorption assays for humoral immunity to cultured autologous melanoma cells. *Proc. Natl. Acad. Sci. USA* **73:**3278–3282
6. Chandy, K., DeCoursey, T., Cahalan, M., McLaughlin, D., Gupta, S. 1984. Voltage gated potassium channels are required for human T lymphocyte activation. *J. Exp. Med.* **160:**369–385
7. Day, M.L., Pickering, S.J., Johnson, M.H., Cook, D.I. 1993. Cell-cycle control of a large-conductance K^+ channel in mouse early embryos. *Nature* **365:**560–562
8. DeCoursey, T.E., Chandy, K.G., Gupta, S., Cahalan, M.D. 1985. Voltage-gated K^+ channels in human T lymphocytes: a role in mitogenesis? *Nature* **307:**465–468
9. Dotsika, E.N., Sanderson, C.J. 1987. A fluorometric assay for determining cell growth in lymphocyte proliferation and lymphokine assays. *J. Immunol. Meth.* **105:**55–62
10. Findlay, I., Dunne, M.J., Petersen, O.H. 1985. High-conductance K^+ channel in pancreatic islet cells can be activated and inactivated by internal calcium. *J. Membrane Biol.* **83:**169–175
11. Gelfand, E., Reuven, O. 1991. Charybdotoxin-sensitive Ca^{2+}-dependent membrane potential changes are not involved in human T or B cell activation and proliferation. *J. Immunol.* **147:**3452–3458
12. Grissmer, S., Cahalan, M. 1992. Ca^{2+}-activated K^+ channels in human leukemic T cells. *J. Gen. Physiol.* **99:**63–84
13. Grynkiewicz, G., Poeni, M., Tsien, R.Y. 1985. A new generation of Ca^{2+} indicators with greatly improved fluorescence properties. *J. Biol. Chem.* **260:**3440–3450
14. Henkel, U., Wollina, U., Garbe, K., Krasagakis, K., Organos, C.E. 1992. Calcium/calmodulin stimulation of human melanoma cell growth and differentiation in vitro. *Eur. J. Dermatol.* **2:**273–278
15. Hess, S.D., Oortgiesen, M., Cahalan, M.D. 1993. Calcium oscillations in human T and natural killer cells depend upon membrane potential and calcium influx. *J. Immunol.* **150:**2620–2633
16. Hille, B. 1991. Ionic channels of excitable membranes. pp. 127–135. Sinauer Associates, Sunderland, Massachusetts
17. Hoth, M., Penner, R. 1992. Depletion of intracellular calcium stores activates a calcium current in mast cells. *Nature* **355:**353–356
18. Latorre, R., Oberhauser, A., Labarca, P., Alvarez, O. 1989. Varieties of calcium-activated potassium channels. *Ann. Rev. Physiol.* **51:**385–399
19. Leonard, R.J., Garcia, M.L. Slaughter, R.S., Reuben, J.P. 1992. Selective blockers of voltage-gated K^+ channels depolarize human T lymphocytes: mechanism of the antiproliferative effect of charybdotoxin. *Proc. Natl. Acad. Sci. USA* **89:**10094–10098
20. Lepple-Wienhues, A., Berweck, S., Boehmig, M., Schröder, K., Garbe, C., Wiederholt, M. 1993. Potassium current and proliferation of cultured malignant and normal human melanocytes. *Pfluegers Arch.* **422:**R69 (*Abstr.*)
21. Lepple-Wienhues, A., Berweck, S., Meyling, B., Garbe, C., Wiederholt, M. 1992. Membrane voltage, whole cell current and intracellular calcium in a human melanoma cell line *Pfluegers Arch.* **420:**R65 (*Abstr.*)
22. Lewis, R., Cahalan M. 1990. Ion channels and signal transduction in lymphocytes. *Annu. Rev. Physiol.* **52:**415–430
23. Lin, CS, Botz, R.C., Blake, J.T., Nguyen, M., Talento, A., Fischer, P.A., Springer, M.S., Sigal, N.H., Slaughter, R.S., Garcia, M.L., Kaczorowski, G.J., Koo, G.C. 1993. Voltage-gated potassium channels regulate calcium-dependent pathways involved in human T lymphocyte activation. *J. Exp. Med.* **177:**637–645
24. Neher, E. 1988. The influence of intracellular Ca^{2+} concentration on degranulation of dialyzed mast cells from rat peritoneum. *J. Physiol.* **395:**193–214
25. Nilius, B., Böhm, T., Wohlrab, W. 1990. Properties of a potassium-selective ion channel in human melanoma cells. *Pfluegers Arch.* **417:**269–277
26. Nilius, B., Schwarz, G., Droogmans, G. 1993. Control of intracellular calcium by membrane potential in human melanoma cells. *Am. J. Physiol.* **265:**C1501–C1510
27. Nilius, B., Wohlrab, W. 1992. Potassium channels and regulation of proliferation of human melanoma cells. *J. Physiol.* **445:**537–548
28. Penner, R., Matthews, G., Neher, E. 1988. Regulation of calcium influx by second messengers in rat mast cells. *Nature* **334:**499–504
29. Rae, J.L., Levis, R.A. 1992. A method for exceptionally low noise single channel recordings. *Pfluegers Arch.* **420:**618–620
30. Richardson, D., Baker, E. 1992. The effect of desferrioxamine and ferric ammonium citrate on the uptake of iron by the membrane iron-binding component of human melanoma cells. *Biochim. Biophys. Acta* **31:**275–280
31. Rouzaire-Dubois, B., Dubois, J-M. 1991. A quantitative analysis of the role of K^+ channels in mitogenesis of neuroblastoma cells. *Cellular Signaling* **4:**333–339
32. Teulon, J., Ronco, P.M., Geniteau-Legendre, M., Baudouin, B., Estrade, S., Cassingena, R., Vandewalle, A.J. 1992. Transformation of renal tubule epithelial cells by simian virus-40 is associated with emergence of Ca^{2+}-insensitive K^+ channels and altered mitogenic sensitivity by K^+ channel blockers. *Cell. Physiol.* **151:**113–125
33. Wegman, E.A., Young, J.A., Cook, D.I. 1991. A 23-pS Ca^{2+}-activated K^+ channel in MCF-7 human breast carcinoma cells: an apparent correlation of channel incidence with the rate of cell proliferation. *Pfluegers Arch.* **417:**562–570
34. Zweifach, A., Lewis, R.S. 1993. Mitogen-regulated Ca^{2+} current of T lymphocytes is activated by depletion of intracellular Ca^{2+} stores. *Proc. Natl. Acad. Sci. USA* **90:**6295–6299